Exponential Euler-Maruyama scheme for simulation of stiff biochemical reaction systems

Yoshio Komori[†] and Kevin Burrage[‡,§]

[†]Department of Systems Design and Informatics
Kyushu Institute of Technology

[‡]Department of Computer Science
University of Oxford

[§]Discipline of Mathematics
Queensland University of Technology

[†]680-4 Kawazu
Iizuka, 820-8502, Japan
komori@ces.kyutech.ac.jp

[‡]Wolfson Building
Parks Road, Oxford, UK
[§]Brisbane, Australia
kevin.burrage@cs.ox.ac.uk, kevin.burrage@gmail.com

Abstract

In order to simulate stiff biochemical reaction systems, an explicit exponential Euler-Maruyama scheme is derived for multi-dimensional, non-commutative stochastic differential equations with a semilinear drift term. The scheme is of strong order a half and A-stable in mean square. The combination with this and the projection method shows good performance in numerical experiments dealing with an alternative formulation of the chemical Langevin equation for a human ether a-go-go related gene ion channel model.

1 Introduction

While it has been customary to treat the numerical solution of stiff ordinary differential equations (ODEs) by implicit methods, there are some classes of explicit methods that are well suited to solving some types of stiff problems. One such class is the class of Runge-Kutta Chebyshev (RKC) methods. They are useful for the stiff problems whose eigenvalues lie near the negative real axis. An original contribution is by van der Houwen and Sommeijer [38] who have constructed explicit s-stage Runge-Kutta (RK) methods whose stability functions are shifted Chebyshev polynomials $T_s(1 + z/s^2)$. These have stability regions along the negative real axis of $[-2s^2, 0]$. In order to achieve second or fourth order, this class of methods has been modified by Abdulle and Medovikov [4] and Abdulle [1], respectively. Note that these methods need to increase the stage number s for stabilization. Another suitable class of methods is the class of explicit exponential RK methods for semilinear problems [14, 17, 18, 19, 32]. Although these methods were proposed many years ago, until recently they have not been regarded as practical because of the cost of calculations for matrix exponentials, especially for large problems. In order to overcome this problem, new methods have been proposed [17, 18, 19]. Note that explicit exponential RK methods are A-stable.

Similarly, for stochastic differential equations (SDEs) stabilized explicit RK methods have been developed. An original contribution concerning RKC methods is by Abdulle and his colleagues [2, 3] who have developed a family of explicit stochastic orthogonal Runge-Kutta Chebyshev (SROCK) methods with extended mean square (MS) stability regions. Their methods have strong order a half and weak order one for non-commutative Stratonovich and Itô SDEs, whereas they reduce to the first order RKC methods when applied to ODEs. By developing their ideas, Komori and Burrage [27, 28] have proposed weak second order SROCK methods for non-commutative Stratonovich SDEs and strong first order SROCK methods for non-commutative Itô and Stratonovich SDEs. They reduce to the first or second order RKC methods when applied to ODEs. Note that these methods also need to increase the stage number for stabilization. In addition, a class of exponential integrators for SDEs, known as Local Linearization (LL) methods, have been proposed by Jimenez [22, 23, 24] and Cruz [12] for the strong approximation to solutions of SDEs with additive noise, whereas Biscay [7] and Shoji [34] have considered LL methods for scalar SDEs with multiplicative noise. Mora [30] and Carbonell [10] have also proposed LL methods for the weak approximation to solutions of SDEs with additive noise. In addition, exponential integrators have been considered for stochastic partial differential equations with a semilinear drift term and additive noise [21].

In biochemical kinetics, the chemical Langevin equation (CLE) is an important modelling framework and it plays an intermediate role between the chemical master equation and the reaction rate equation for biochemical simulation [15, 20, 29]. The CLE consists of a system of Itô SDEs with non-commutative noise. In a seminal paper Gillespie [15] has derived an original form of the CLE. Mélykúti, Burrage and Zygalakis [29] have considered other possible forms and have derived a computationally effective form that needs fewer Wiener increments than that in Gillespie's original formulation. In order for simulation of the CLE to be biological meaningful, approximate solutions have to be non-negative and they are often required to satisfy other boundary conditions. Dangerfield, Kay and Burrage [13] have proposed tackling such problems by the use of reflected SDEs [35, 36] and the projection method [11].

In the present paper we shall put all these ideas together. In using projection method, numerical methods with one intermediate stage are the most favourable and so we will derive an explicit exponential Euler-Maruyama (EM) scheme for multi-dimensional, non-commutative Itô SDEs with a semilinear drift term. The method together with the projection method will show very good performance for stiff biochemical problems. In Section 2 we will introduce the exponential Euler scheme for ODEs and derive the exponential EM scheme for SDEs. After that, we will investigate its MS stability. In Section 3 we will introduce reflected SDEs and the projection method. Section 4 will present numerical results and Section 5 our conclusions.

2 Exponential schemes

2.1 Exponential Euler scheme

We consider autonomous semilinear ODEs given by

$$\boldsymbol{y}'(t) = A\boldsymbol{y}(t) + \boldsymbol{f}(\boldsymbol{y}(t)), \qquad t > 0, \qquad \boldsymbol{y}(0) = \boldsymbol{y}_0, \tag{2. 1}$$

where $\boldsymbol{y}$ is an $\mathbb{R}^d$-valued function on $[0, \infty)$, A is a $d \times d$ matrix and $\boldsymbol{f}$ is an $\mathbb{R}^d$-valued nonlinear function on $\mathbb{R}^d$ or a constant vector. By the variation-of-constants formula, the exact solution of (2. 1) is represented as

$$\boldsymbol{y}(t) = \mathrm{e}^{At}\boldsymbol{y}_0 + \int_0^t \mathrm{e}^{A(t-s)}\boldsymbol{f}(\boldsymbol{y}(s))\mathrm{d}s. \tag{2. 2}$$

When $\boldsymbol{y}_n$ denotes a discrete approximation to the solution $\boldsymbol{y}(t_n)$ of (2. 1) for an equidistant grid point $t_n \overset{\text{def}}{=} nh$ ($n = 1, 2, \ldots, M$) with step size h (M is a natural number), we can derive a numerical scheme by utilizing (2. 2). From (2. 2), we have

$$\boldsymbol{y}(t_{n+1}) = \mathrm{e}^{Ah}\boldsymbol{y}_n + \int_{t_n}^{t_{n+1}} \mathrm{e}^{A(t_{n+1}-s)}\boldsymbol{f}(\boldsymbol{y}(s))\mathrm{d}s$$

if $\boldsymbol{y}(t_n) = \boldsymbol{y}_n$. By interpolating $\boldsymbol{f}(\boldsymbol{y}(s))$ at $\boldsymbol{f}(\boldsymbol{y}_n)$ only, we obtain the simplest exponential scheme for (2. 1) [19]:

$$\boldsymbol{y}_{n+1} = \mathrm{e}^{Ah}\boldsymbol{y}_n + A^{-1}\left(\mathrm{e}^{Ah} - I\right)\boldsymbol{f}(\boldsymbol{y}_n), \tag{2. 3}$$

where I stands for the $d \times d$ identity matrix. This is called the exponential Euler scheme.

When we apply (2. 3) to the scalar test equation

$$y'(t) = \lambda y(t), \quad t > 0, \quad y(0) = y_0, \tag{2. 4}$$

where $\Re(\lambda) \leq 0$ and $y_0 \neq 0$, we have $y_{n+1} = R(\lambda h)y_n$ for which $R(z) = \mathrm{e}^z$. Thus, although (2. 3) is an explicit scheme, it is A-stable, that is, its stability region $\{z \mid |R(z)| \leq 1\}$ contains the whole left half of the complex plane [9].

2.2 Exponential EM scheme

Similarly to the previous subsection, we are concerned with autonomous SDEs with the semilinear drift term given by

$$\mathrm{d}\boldsymbol{y}(t) = (A\boldsymbol{y}(t) + \boldsymbol{f}(\boldsymbol{y}(t)))\mathrm{d}t + \sum_{j=1}^{m} \boldsymbol{g}_j(\boldsymbol{y}(t))\mathrm{d}W_j(t), \qquad t > 0, \qquad \boldsymbol{y}(0) = \boldsymbol{y}_0, \quad (2.\ 5)$$

where $\boldsymbol{g}_j$, $j = 1, 2, \ldots, m$ are $\mathbb{R}^d$-valued functions on $\mathbb{R}^d$, the $W_j(t)$, $j = 1, 2, \ldots, m$ are independent Wiener processes and $\boldsymbol{y}_0$ is independent of $W_j(t) - W_j(0)$ for $t > 0$. If a global Lipschitz condition is satisfied, the stochastic differential equation (SDE) has exactly one continuous global solution on the entire interval $[0, \infty)$ [5, p. 113].

Similarly to (2. 1), the exact solution of (2. 5) is represented by

$$\boldsymbol{y}(t) = \mathrm{e}^{At}\boldsymbol{y}_0 + \int_0^t \mathrm{e}^{A(t-s)}\boldsymbol{f}(\boldsymbol{y}(s))\mathrm{d}s + \sum_{j=1}^{m} \int_0^t \mathrm{e}^{A(t-s)}\boldsymbol{g}_j(\boldsymbol{y}(s))\mathrm{d}W_j(s). \qquad (2.\ 6)$$

By utilizing (2. 6), we can have an approximation to $\boldsymbol{y}(t_{n+1})$ as follows:

$$\boldsymbol{y}(t_{n+1}) \simeq \mathrm{e}^{Ah}\boldsymbol{y}_n + A^{-1}\left(\mathrm{e}^{Ah} - I\right)\boldsymbol{f}(\boldsymbol{y}_n) + \sum_{j=1}^{m}\left(\int_{t_n}^{t_{n+1}} \mathrm{e}^{A(t_{n+1}-s)}\mathrm{d}W_j(s)\right)\boldsymbol{g}_j(\boldsymbol{y}_n)$$

if $\boldsymbol{y}(t_n) = \boldsymbol{y}_n$. In [34], another approximation was considered for scalar SDEs. In order to approximate the stochastic integrals in the right-hand side, let us consider an approximation

$$\int_{t_n}^{t_{n+1}} \alpha\mathrm{d}W_j(s) \qquad (2.\ 7)$$

to $\int_{t_n}^{t_{n+1}} \mathrm{e}^{a(t_{n+1}-s)}\mathrm{d}W_j(s)$, where $a \in \mathbb{R}$. Because its MS error is given by

$$E\left[\left\{\int_{t_n}^{t_{n+1}}\left(\mathrm{e}^{a(t_{n+1}-s)} - \alpha\right)\mathrm{d}W_j(s)\right\}^2\right] = \int_{t_n}^{t_{n+1}}\left(\mathrm{e}^{a(t_{n+1}-s)} - \alpha\right)^2\mathrm{d}s,$$

by differentiating this with respect to α and setting it at zero, we obtain

$$\alpha = (ah)^{-1}\left(\mathrm{e}^{ah} - 1\right). \qquad (2.\ 8)$$

Hence, we can derive the following exponential EM scheme:

$$\boldsymbol{y}_{n+1} = \mathrm{e}^{Ah}\boldsymbol{y}_n + A^{-1}\left(\mathrm{e}^{Ah} - I\right)\boldsymbol{f}(\boldsymbol{y}_n) + (Ah)^{-1}\left(\mathrm{e}^{Ah} - I\right)\sum_{j=1}^{m}\triangle W_j\boldsymbol{g}_j(\boldsymbol{y}_n). \qquad (2.\ 9)$$

In general, when discrete approximations $\boldsymbol{y}_n$ are given by a numerical scheme, we say that the scheme is of strong order p if there exists a constant C such that

$$\left(E[||\boldsymbol{y}_M - \boldsymbol{y}(T)||^2]\right)^{1/2} \leq Ch^p$$

with $T = Mh$ and h sufficiently small [26, 33], where $||\cdot||$ stands for the Euclidean norm. Let us assume $\boldsymbol{f}, \boldsymbol{g}_j \in \boldsymbol{C}^2$ for $j = 1, 2, \ldots, m$. Then, it is known that the EM scheme

$$\boldsymbol{y}_{n+1} = \boldsymbol{y}_n + h(A\boldsymbol{y}_n + \boldsymbol{f}(\boldsymbol{y}_n)) + \sum_{j=1}^{m}\triangle W_j\boldsymbol{g}_j(\boldsymbol{y}_n) \qquad (2.\ 10)$$

is of strong order a half [26, 33].

The following points can be made.

- When A goes to the zero matrix, (2. 9) is equivalent to the EM scheme.

- Because the expression on the right-hand side of (2. 9) can be truncated in the following form

$$\boldsymbol{y}_{n+1} = \boldsymbol{y}_n + h(A\boldsymbol{y}_n + \boldsymbol{f}(\boldsymbol{y}_n)) + \sum_{j=1}^{m} \triangle W_j \boldsymbol{g}_j(\boldsymbol{y}_n)$$

$$+ \frac{1}{2}h^2 A(A\boldsymbol{y}_n + \boldsymbol{f}(\boldsymbol{y}_n)) + \frac{1}{2}h \sum_{j=1}^{m} \triangle W_j A\boldsymbol{g}_j(\boldsymbol{y}_n)$$

for a small h, (2. 9) is also of strong order a half.

- It is reasonable to approximate $e^{a(t_{n+1}-s)}$ by the constant α in (2. 7) as even $\int_{t_n}^{t_{n+1}} s\mathrm{d}W_j(s)$ is of order one and a half in MS.

- For (2. 8), (2. 7) obeys the normal distribution with mean 0 and variance

$$\int_{t_n}^{t_{n+1}} \alpha^2 \mathrm{d}s = \frac{1}{a^2 h}\left(e^{ah} - 1\right)^2 = h + ah^2 + \frac{7}{12}a^2 h^3 + O(h^4),$$

whereas $\int_{t_n}^{t_{n+1}} e^{a(t_{n+1}-s)}\mathrm{d}W_j(s)$ obeys the normal distribution with mean 0 and variance

$$\int_{t_n}^{t_{n+1}} e^{2a(t_{n+1}-s)}\mathrm{d}s = \frac{1}{2a}\left(e^{2ah} - 1\right) = h + ah^2 + \frac{2}{3}a^2 h^3 + O(h^4)$$

(see also [34]).

2.3 MS stability analysis for the exponential EM scheme

As with the deterministic case, if we apply (2. 9) to the scalar test equation [16]

$$\mathrm{d}y(t) = \lambda y(t)\mathrm{d}t + \sum_{j=1}^{m} \sigma_j y(t)\mathrm{d}W_j(t), \qquad t > 0, \qquad y(0) = y_0, \qquad (2.\ 11)$$

where $y_0 \neq 0$ with probability one (w. p. 1) and where the complex coefficients satisfy

$$2\Re(\lambda) + \sum_{j=1}^{m} |\sigma_j|^2 < 0, \qquad (2.\ 12)$$

then, we have

$$y_{n+1} = R\left(\lambda h, \sum_{j=1}^{m} \sigma_j \triangle W_j\right) y_n$$

for which $R(z, w) = e^z + z^{-1}(e^z - 1)w$.

Because of (2. 12), the solution of (2. 11) is MS stable ($\lim_{t\to\infty} E[|y(t)|^2] = 0$) [16]. On the other hand, the MS stability function $\hat{R}$ of (2. 9) is given by

$$\hat{R}(p_r, p_i, q) \overset{\text{def}}{=} E\left[\left|R\left(\lambda h, \sum_{j=1}^{m} \sigma_j \triangle W_j\right)\right|^2\right] = e^{2p_r} + \frac{(e^{2p_r} - 2e^{p_r}\cos p_i + 1)\,q}{p_r^2 + p_i^2} \qquad (2.\ 13)$$

4

where $p_r \overset{\text{def}}{=} \Re(\lambda)h$, $p_i \overset{\text{def}}{=} \Im(\lambda)h$ and $q \overset{\text{def}}{=} \sum_{j=1}^{m} |\sigma_j|^2 h$. The MS stability $(E[|y_n|^2] \to 0$ $(n \to \infty))$ for (2. 9) is equivalent to $\hat{R}(p_r, p_i, q) < 1$ [16]. Thus, the MS stability domain of (2. 9) is defined by $\{(p_r, p_i, q) \mid \hat{R}(p_r, p_i, q) < 1\}$.

We can rewrite (2. 12) as $2p_r + q < 0$. Using this, we obtain

$$\hat{R}(p_r, p_i, q) < e^{2p_r} - \frac{2p_r \left(e^{2p_r} - 2e^{p_r} \cos p_i + 1\right)}{p_r^2 + p_i^2}, \tag{2. 14}$$

from (2. 13). Denote by $\varphi(p_r, p_i)$ the expression in the right-hand side.

First, let us consider the case of $p_i = 0$. As

$$\varphi(p_r, 0) = \frac{(p_r - 2)e^{2p_r} + 4e^{p_r} - 2}{p_r},$$

we have $\lim_{p_r \to -0} \varphi(p_r, 0) = 1$ and $\varphi(p_r, 0)$ is a monotone increasing function of p_r. Thus, $\hat{R}(p_r, 0, q) < 1$ for $p_r < 0$ under the condition (2. 12).

Next, let us consider the case of $p_i \geq \pi$. In this case, we have

$$\varphi(p_r, \pi) \leq \frac{(p_r^2 - 2p_r + \pi^2)e^{2p_r} - 4p_r e^{p_r} - 2p_r}{p_r^2 + \pi^2}.$$

When we denote by $\psi_1(p_r)$ the expression in the right-hand side, we have $\psi_1(0) = 1$ and

$$\psi_1'(p_r) = 2\frac{\left\{(p_r^2 + \pi^2 + \pi)\, e^{p_r} - p_r + \pi\right\} u(p_r) - 2p_r \left(p_r^2 + \pi^2\right) e^{2p_r} + p_r^2 \left(e^{p_r} + 2\right) e^{p_r}}{\left(p_r^2 + \pi^2\right)^2},$$

where

$$u(p_r) \overset{\text{def}}{=} \left(p_r^2 + \pi^2 - \pi\right) e^{p_r} - p_r - \pi.$$

As $u'(0) > 0$, $\lim_{p_r \to -\infty} u'(p_r) = -1$ and $u''(p_r) > 0$, $u(p_r)$ is a convex function and it reaches its minimum value at a point, say, β, in the interval $(-\infty, 0]$. We can numerically obtain $\beta = -1.869$ and $u(\beta) = 0.304$. Thus, $u(p_r) > 0$ holds for $p_r \leq 0$. This fact leads to $\hat{R}(p_r, p_i, q) < 1$ for $p_r \leq 0$ and $p_i \geq \pi$ under the condition (2. 12).

As $\hat{R}(p_r, p_i, q) = \hat{R}(p_r, -p_i, q)$, all that remains is the case of $\pi > p_i > 0$. Denote by $\psi_2(p_r)$ $\varphi(p_r, \varepsilon)$ for a positive $\varepsilon < \pi$. Then, since $\psi_2'(p_r) > 0$ for $p_r \leq -\varepsilon$, we have $\psi_2(p_r) \leq \psi_2(-\pi)$ for $p_r \leq -\pi$, which implies $\varphi(p_r, \varepsilon) \leq \varphi(-\pi, \varepsilon)$. On the other hand, $\varphi(-\pi, p_i)$ is a monotone decreasing function of p_i when $0 < p_i < \pi$, and $\varphi(-\pi, 0) < 1$. Thus, $\hat{R}(p_r, p_i, q) < 1$ for $p_r \leq -\pi$ and $0 < p_i < \pi$ under the condition (2. 12). Consequently, we plot the MS stability domain for $0 < p_r < -\pi$ and $0 < p_i < \pi$.

The MS stability domain and its profiles are given in Figure 1. The MS stability domain is indicated by the colored part in the top left of the figure. Here, the other part enclosed by the mesh indicates the domain in which the solution of the test SDE is MS stable. In the bottom of the figure, the dark-colored area indicates the profile of the MS stability domain when $p_i = 0$, 0.125 or 0.25, whereas the area enclosed by the two straight lines $q = 0$ and $q = -2p_r$ indicates the region in which the solution of the test SDE is MS stable. In the top right of the figure, the dark-colored area indicates the profile of the MS stability domain when $q = -2p_r$, which is the boundary of the stability region of the test SDE. From these results, we can see that the exponential EM scheme is A-stable in MS [16], that is, its stability domain contains the domain that satisfies $2p_r + q < 0$.
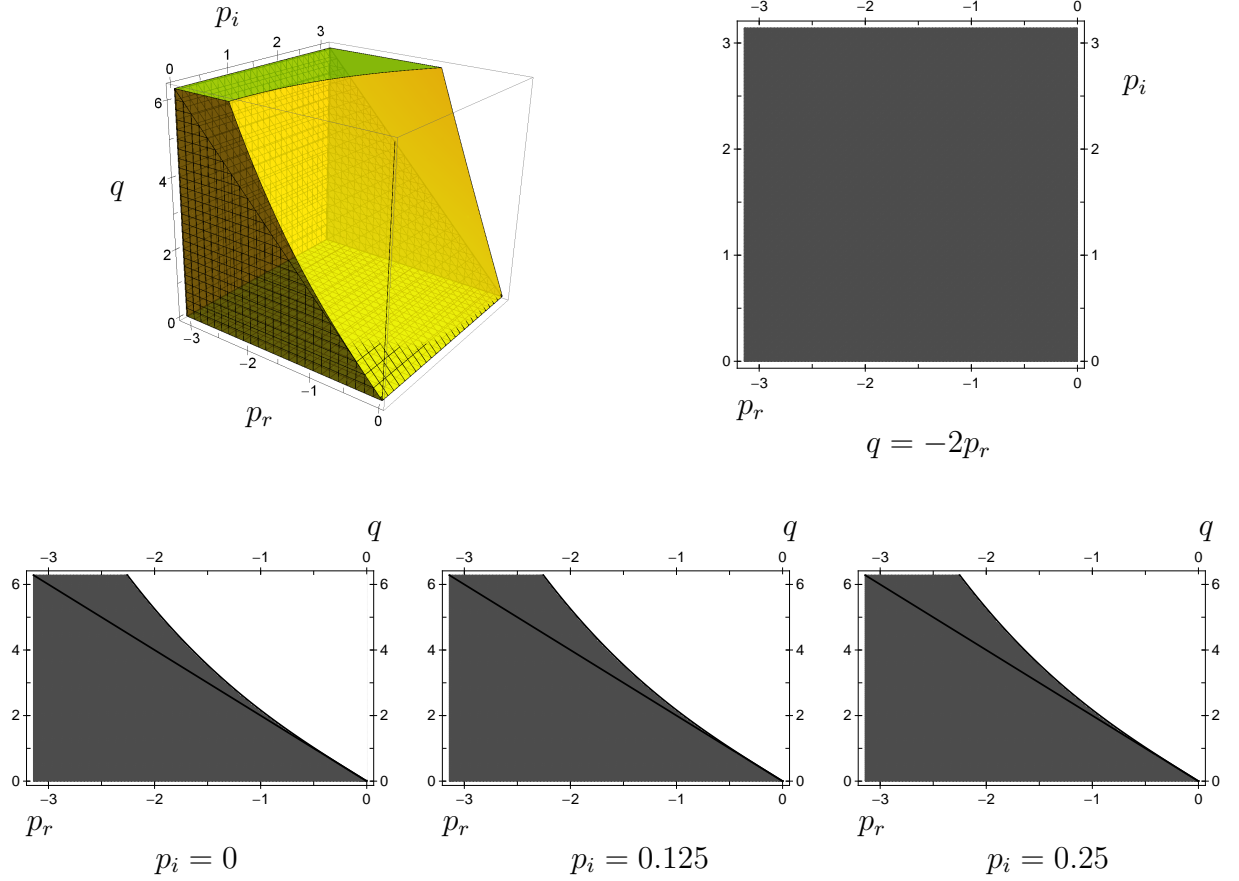
Figure 1: MS stability domain (top left) and its profiles (top right and bottom) for the exponential EM scheme

For comparisons, lastly let us check the stability of the EM scheme. When (2. 10) is applied to (2. 11), the MS stability function of (2. 10) is given by

$$\hat{R}(p_r, p_i, q) = (1 + p_r)^2 + p_i^2 + q.$$

The MS stability domain and its profile are given in Figures 2. In the profile, the light-colored area indicates the region in which the solution of the test SDE is MS stable, but which is not included in the MS stability domain.

3 Reflected SDEs and projection method

3.1 Reflected SDEs

When (2. 5) is considered for biological simulation, one of the critical problems often leads to keeping the non-negativity of each component of the solution and conserving the sum of the components because of having biological meaning – the components of them represent chemical concentrations. In order to overcome the problem, Dangerfield et al. [13] have proposed using reflected SDEs instead of directly using (2. 5). In this subsection, we briefly review the concept of reflected SDEs.

For the solution of (2. 5), we require that $0 \leq y_i(t) \leq L$ $(i = 1, 2, \ldots, d)$ and $\sum_{i=1}^{d} y_i(t) = L$ for an $L > 0$. Then, $\boldsymbol{y}(t)$ is restricted to the hyperplane given by
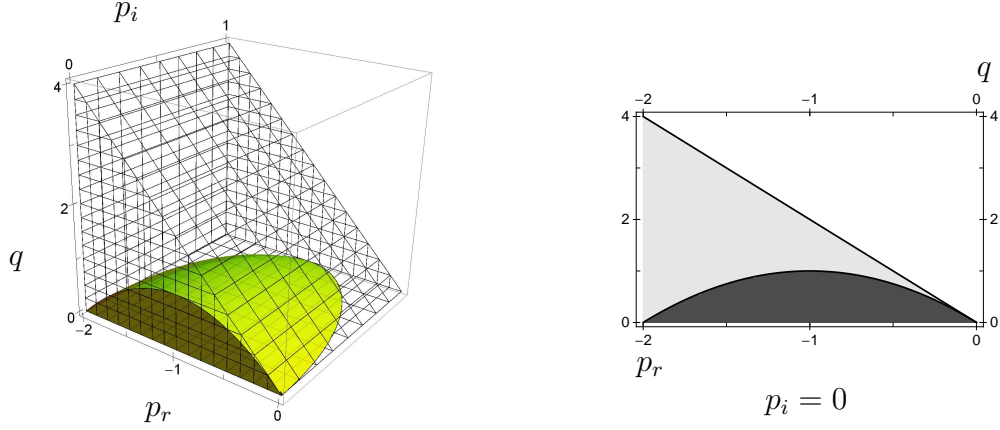
Figure 2: MS stability domain (left) and its profile (right) for the EM scheme

$\sum_{i=1}^{d} y_i(t) = L$ which lies inside the hypercube bounded by the intervals $[0, L]$. In what follows, we denote by D the hyperplane, that is, the reflected domain of the process $\boldsymbol{y}(t)$.

For $\boldsymbol{y}(t)$ to remain on D, we decompose it into the sum of two processes such as $\boldsymbol{y}(t) = \boldsymbol{x}(t) + \boldsymbol{r}(t)$. Here, $\boldsymbol{x}(t)$ satisfies (2. 5) and describes the behavior of $\boldsymbol{y}(t)$ on the interior of D, that is, $\boldsymbol{y}(0) = \boldsymbol{x}(0)$ and $\boldsymbol{y}(t) = \boldsymbol{x}(t)$ on D. On the other hand, $\boldsymbol{r}(t)$ determines the behavior of $\boldsymbol{y}(t)$ on the boundary of D, say ∂D, and reflects $\boldsymbol{y}(t)$ into D. As the measure induced by $\boldsymbol{r}(t)$ must be concentrated at the time t_e for which $\boldsymbol{y}(t_e) \in \partial D$, the following property is required [6, 13]:

$$|\boldsymbol{r}|(t) = \int_0^t \mathbf{1}_{\{\boldsymbol{y}(s) \in \partial D\}} \mathrm{d}|\boldsymbol{r}|(s). \tag{3. 1}$$

In addition, for $\boldsymbol{r}(t)$ to reflect $\boldsymbol{y}(t)$ into D in the direction of the inward pointing unit normal, the following property is also required [13]:

$$\boldsymbol{r}(t) = \int_0^t \nu(s) \mathrm{d}|\boldsymbol{r}|(s), \tag{3. 2}$$

where $\nu(s) \in N(\boldsymbol{y}(s))$ if $\boldsymbol{y}(s) \in \partial D$ and $N(\boldsymbol{a})$ is the set of inward pointing unit vectors to the point $\boldsymbol{a}$ that lies on ∂D. After all, with (3. 1) and (3. 2) we have

$$\mathrm{d}\boldsymbol{y}(t) = (A\boldsymbol{y}(t) + \boldsymbol{f}(\boldsymbol{y}(t)))\mathrm{d}t + \sum_{j=1}^{m} \boldsymbol{g}_j(\boldsymbol{y}(t))\mathrm{d}W_j(t) + \mathrm{d}\boldsymbol{r}(t), \qquad t > 0,$$
$$\boldsymbol{y}(0) = \boldsymbol{y}_0. \tag{3. 3}$$

This SDE is called a reflected SDE [35, 36]. The solution of (3. 3) will be a pair $(\boldsymbol{y}(t), \boldsymbol{r}(t))$ that satisfies (3. 1) and (3. 2) [31, 37]. As a numerical method to solve reflected SDEs, Dangerfield et al. [13] have adopted the projection method. In the next subsection, we will see what it is and how it is used.

3.2 Projection method for reflected SDEs

The projection method is described as follows. When we have an approximate solution $\boldsymbol{y}_n \in D$ at time t_n, from this we calculate an unreflected approximate solution, say $\boldsymbol{y}_{n+1}^{(un)}$,

7

by using the EM scheme or the exponential EM scheme. If $\boldsymbol{y}_{n+1}^{(un)} \in D$, we use this as an approximate solution $\boldsymbol{y}_{n+1}$ at time t_{n+1}. If not, we use the projection of $\boldsymbol{y}_{n+1}^{(un)}$ onto ∂D. When $\Pi(\cdot)$ denotes the projection, this procedure can be rewritten as

$$\boldsymbol{y}_{n+1} = \begin{cases} \boldsymbol{y}_{n+1}^{(un)} & \text{if } \boldsymbol{y}_{n+1}^{(un)} \in D, \\ \Pi(\boldsymbol{y}_{n+1}^{(un)}) & \text{if } \boldsymbol{y}_{n+1}^{(un)} \notin D. \end{cases}$$

Although we have not explicitly written calculations for the reflecting process $\boldsymbol{r}(t)$ here, if we want to do it, note that it can be written as

$$\boldsymbol{r}_0 = 0, \qquad \boldsymbol{r}_{n+1} = \begin{cases} \boldsymbol{r}_n & \text{if } \boldsymbol{y}_{n+1}^{(un)} \in D, \\ \boldsymbol{r}_n + \Pi(\boldsymbol{y}_{n+1}^{(un)}) - \boldsymbol{y}_{n+1}^{(un)} & \text{if } \boldsymbol{y}_{n+1}^{(un)} \notin D. \end{cases}$$

The projection Π can be described as follows [11]: for any given vector $\boldsymbol{y} \in \mathbb{R}^d$, the projection of $\boldsymbol{y}$ onto D is to solve the minimization problem

$$\boldsymbol{u} = \arg \min_{\boldsymbol{x} \in D} ||\boldsymbol{x} - \boldsymbol{y}||.$$

Using the Moreau's identity, Chen and Ye [11] have shown that the problem can be simplified to a univariate minimization problem. Furthermore, they have shown that there are d possible candidates which can be computed explicitly and $\boldsymbol{u}$ is the only one of these that falls into D. After all, the algorithm that gives $\Pi(\boldsymbol{y}_{n+1}^{(un)})$ is as follows [11, 13]:

1) Set $\boldsymbol{u} := \boldsymbol{y}_{n+1}$, where $\boldsymbol{y}_{n+1}$ is an approximate solution to (2. 5) calculated by the EM scheme or the exponential EM scheme.

2) Sort the elements of $\boldsymbol{u}$ in the ascending order as $u_{(1)} \le u_{(2)} \le \cdots \le u_{(d)}$, and set $i := d - 1$.

3) Set s_i by

$$s_i := \frac{1}{d - i} \left(\sum_{k=i+1}^{d} u_{(k)} - K \right).$$

If $s_i \ge u_{(i)}$, then set $\hat{s} := s_i$ and go to Step 5). Otherwise, set $i := i - 1$ and redo Step 3) if $i \ge 1$ or go to Step 4) if $i = 0$.

4) Set $\hat{s}$ by

$$\hat{s} := \frac{1}{d} \left(\sum_{k=1}^{d} u_{(k)} - K \right).$$

5) Return
$$[\max(u_1 - \hat{s}, 0) \ \max(u_2 - \hat{s}, 0) \ \cdots \ \max(u_d - \hat{s}, 0)]^\top$$
as the projection of $\boldsymbol{u}$, where $u_1, u_2, \ldots, u_d$ are the unsorted elements of $\boldsymbol{u}$.

4 Simulation for a K^+ channel

As an example of real interest to biologists, we consider a model for a human ether a-go-go related gene K^+ ion channel [8, 25]. Mélykúti et al. [29] have given the Langevin formulation of this model. The model has three closed states, one open state and one inactivation state as five chemical species reacting through ten reactions, and takes the form

$$
A = \begin{bmatrix}
-k_1 & k_2 & 0 & 0 & 0 \\
k_1 & -k_2 - k_3 & k_4 & 0 & 0 \\
0 & k_3 & -k_4 - k_5 - k_{10} & k_6 & k_9 \\
0 & 0 & k_5 & -k_6 - k_7 & k_8 \\
0 & 0 & k_{10} & k_7 & -k_8 - k_9
\end{bmatrix}, \qquad (4.\ 1)
$$

$$
\boldsymbol{f}(\boldsymbol{y}) = \begin{bmatrix} 0 & 0 & 0 & 0 & 0 \end{bmatrix}^\top,
$$

$$
\begin{bmatrix} \boldsymbol{g}_1(\boldsymbol{y}) & \boldsymbol{g}_2(\boldsymbol{y}) & \boldsymbol{g}_3(\boldsymbol{y}) & \boldsymbol{g}_4(\boldsymbol{y}) & \boldsymbol{g}_5(\boldsymbol{y}) \end{bmatrix}
$$

$$
= \begin{bmatrix}
-1 & 0 & 0 & 0 & 0 \\
1 & -1 & 0 & 0 & 0 \\
0 & 1 & -1 & 0 & 1 \\
0 & 0 & 1 & -1 & 0 \\
0 & 0 & 0 & 1 & -1
\end{bmatrix} \operatorname{diag} \begin{pmatrix}
\sqrt{k_1 y_1 + k_2 y_2} \\
\sqrt{k_3 y_2 + k_4 y_3} \\
\sqrt{k_5 y_3 + k_6 y_4} \\
\sqrt{k_7 y_4 + k_8 y_5} \\
\sqrt{k_9 y_5 + k_{10} y_3}
\end{pmatrix}
$$

with the conditions $0 \le y_i(t) \le L$ $(i = 1, 2, \ldots, 5)$ and

$$
\sum_{i=1}^5 y_i(t) = L, \qquad (4.\ 2)
$$

where $L = \sum_{i=1}^5 y_i(0)$.

Because the rank of A is four in (4. 1), we cannot apply (2. 9) to this formulation. We have to reduce the number of state variables.

4.1 State space reduction

When we set U as

$$
U \stackrel{\text{def}}{=} \begin{bmatrix}
1 & 0 & 0 & 0 & 0 \\
0 & 1 & 0 & 0 & 0 \\
0 & 0 & 1 & 0 & 0 \\
0 & 0 & 0 & 1 & 0 \\
1 & 1 & 1 & 1 & 1
\end{bmatrix},
$$

left multiplication by U does not change the first four rows of A and

$$
[\boldsymbol{g}_1(\boldsymbol{y})\ \boldsymbol{g}_2(\boldsymbol{y})\ \boldsymbol{g}_3(\boldsymbol{y})\ \boldsymbol{g}_4(\boldsymbol{y})\ \boldsymbol{g}_5(\boldsymbol{y})],
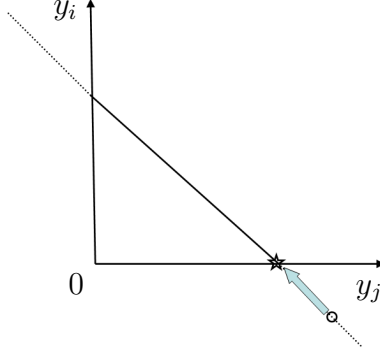$$

Figure 3: Diagrammatical representation of how the projection method works for our formulation

but it makes the last row vanish. This fact leads to the following equivalent formulation with a smaller number of state variables:

$$
A = \begin{bmatrix}
-k_1 & k_2 & 0 & 0 \\
k_1 & -k_2 - k_3 & k_4 & 0 \\
-k_9 & k_3 - k_9 & -k_4 - k_5 - k_9 - k_{10} & k_6 - k_9 \\
-k_8 & -k_8 & k_5 - k_8 & -k_6 - k_7 - k_8
\end{bmatrix},
$$

$$
\boldsymbol{f}(\boldsymbol{y}) = \begin{bmatrix} 0 & 0 & k_9 L & k_8 L \end{bmatrix}^\top, \qquad \boldsymbol{y} = \begin{bmatrix} y_1 & y_2 & y_3 & y_4 \end{bmatrix}^\top,
$$

$$
\begin{bmatrix} \boldsymbol{g}_1(\boldsymbol{y}) & \boldsymbol{g}_2(\boldsymbol{y}) & \boldsymbol{g}_3(\boldsymbol{y}) & \boldsymbol{g}_4(\boldsymbol{y}) & \boldsymbol{g}_5(\boldsymbol{y}) \end{bmatrix}
$$

$$
= \begin{bmatrix}
-1 & 0 & 0 & 0 & 0 \\
1 & -1 & 0 & 0 & 0 \\
0 & 1 & -1 & 0 & 1 \\
0 & 0 & 1 & -1 & 0
\end{bmatrix} \mathrm{diag} \begin{pmatrix}
\sqrt{k_1 y_1 + k_2 y_2} \\
\sqrt{k_3 y_2 + k_4 y_3} \\
\sqrt{k_5 y_3 + k_6 y_4} \\
\sqrt{k_7 y_4 + k_8 (L - \sum_{i=1}^4 y_i)} \\
\sqrt{k_9 (L - \sum_{i=1}^4 y_i) + k_{10} y_3}
\end{pmatrix}
$$

with $y_5(t) = L - \sum_{i=1}^4 y_i(t)$.

As (4. 2) is always satisfied in this formulation, the projection method will be used to keep the non-negativity of the components of the solution. Figure 3 indicates how the projection method works at a certain time step for this formulation. The oblique solid or dotted line represents the hyperplane given by (4. 2). The round point is the value at some time step of the unreflected process, which has a negative i-th component. The star point is the projection of this point onto D.

4.2   Numerical experiments

In order to see how well the exponential EM scheme behaves, we perform numerical experiments. Because the dimension of the matrix A is not too large in our problems, we can diagonalize the matrix [19] for numerical calculations. Assume that we have a diagonal matrix Λ and a diagonalization matrix R such that

$$
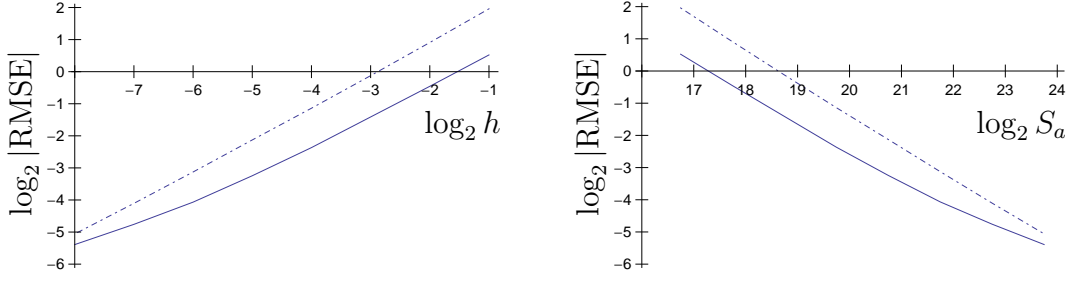\Lambda = \mathrm{diag}(\lambda_1, \lambda_2, \lambda_3, \lambda_4), \qquad AR = R\Lambda.
$$

Figure 4: RMSEs of $\boldsymbol{y}(5)$. (Solid: Exp. EM, dash-dotted: EM.)

Then, in (2. 9) we have

$$\mathrm{e}^{Ah} = R\mathrm{diag}\left(\mathrm{e}^{\lambda_1 h}, \mathrm{e}^{\lambda_2 h}, \mathrm{e}^{\lambda_3 h}, \mathrm{e}^{\lambda_4 h}\right) R^{-1},$$

$$A^{-1}\left(\mathrm{e}^{Ah} - I\right) = R\mathrm{diag}\left(\frac{\mathrm{e}^{\lambda_1 h} - 1}{\lambda_1}, \frac{\mathrm{e}^{\lambda_2 h} - 1}{\lambda_2}, \frac{\mathrm{e}^{\lambda_3 h} - 1}{\lambda_3}, \frac{\mathrm{e}^{\lambda_4 h} - 1}{\lambda_4}\right) R^{-1}.$$

Note that once we calculate these for a given h, we can use them for every step and trajectory.

In the sequel, we investigate the root mean square error (RMSE) by simulating 1000 independent trajectories for a given h. We also investigate computational costs. In the simulation results, we will indicate $S_a \overset{\text{def}}{=} n_e + n_r$, where n_e and n_r stand for the number of evaluations on the drift or diffusion coefficients and the number of generated pseudo random numbers, respectively. As we do not know the exact solution of the SDE in our problem, we will seek a numerical solution by the Milstein scheme [26] with $h = 2^{-10}$ and use it instead of the exact solution [33]. The Milstein scheme will be used only for this because it is very costly in our problem due to approximations to stochastic double integrals and the derivatives of the diffusion coefficients.

The first is a case in which many reflections occur. We set parameters and an initial condition as follows:

$$k_1 = 0.2, \quad k_2 = \frac{k_1}{50}, \quad k_i = k_1 \quad (i = 3, 4, \ldots, 10),$$
$$\boldsymbol{y}_0 = [100\ 50\ 100\ 50\ 100]^\top \quad (\text{w. p. } 1).$$

The root mean square errors (RMSEs) are indicated in Figure 4. As the solution is a vector, the Euclidean norm is used. The solid or dash-dotted lines denote the exponential EM scheme or the EM scheme, respectively. We can see that the exponential EM scheme is better. On the other hand, Figure 5 indicates the number of reflections per step over 1000 trajectories. We can see that there is not a large difference in the number of reflections.

The second problem is a stiff one depending on the value of k_1. We set the other parameters as follows:

$$k_2 = k_1, \quad k_i = 0.5 \quad (i = 3, 4, \ldots, 10).$$

The initial condition is the same as the previous case. For several values of k_1, RMSEs are indicated in Figure 6. As k_1 becomes large, the SDE becomes increasingly stiff. When $k_1 = 50$,
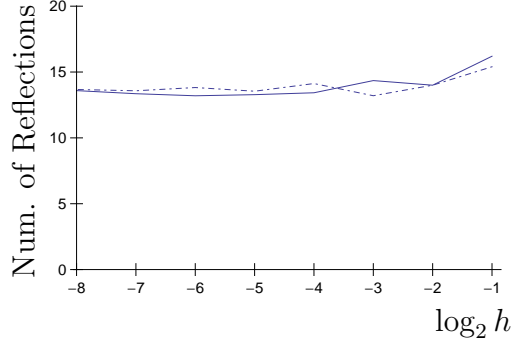
11

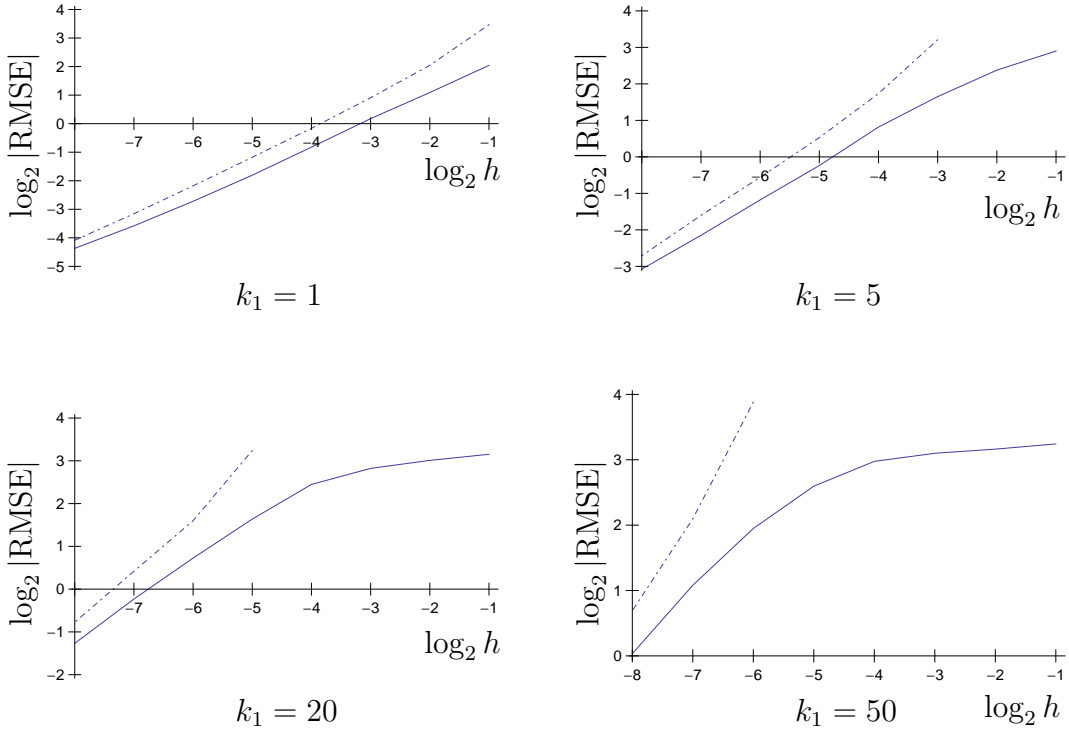Figure 5: Number of reflections per step over 1000 trajectories. (Solid: Exp. EM, dash-dotted: EM.)

Figure 6: RMSEs of $\boldsymbol{y}(5)$ for several values of k_1. (Solid: Exp. EM, dash-dotted: EM.)

for example, we need a small step size h for the EM scheme to solve the SDE numerically stably. This is because one of the eigenvalues of A is -100.252. (Remember Figure 2.) On the other hand, for the exponential EM scheme we do not need such a small h as it is A-stable. Incidentally, Figure 7 indicates the RMSE versus the computational cost and the number of reflections when $k_1 = 50$. From these results, we can see that the exponential EM scheme has good performance not only with respect to stability, but also in terms of computational costs.
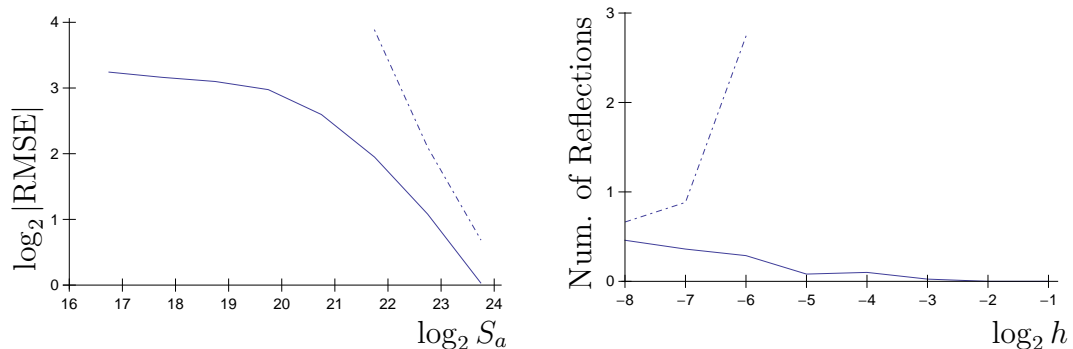
12

Figure 7: RMSEs of $\boldsymbol{y}(5)$ and the number of reflections per step over 1000 trajectories when $k_1 = 50$. (Solid: Exp. EM, dash-dotted: EM.)

5 Conclusions

For non-commutative Itô SDEs with the semilinear drift term, we have derived the exponential EM scheme, which is of strong order a half. Using the scalar test SDE with complex coefficients, we have investigated stability properties for the scheme and have shown that it is A-stable in MS.

For the numerical experiments we have dealt with the model for a K^+ channel that is computationally efficient [13], and have carried out the state space reduction for it. Then, using the reflection technique to keep the non-negativity of the numerical solutions, we have confirmed the advantages of the exponential EM scheme in the numerical experiments. Whereas the EM scheme has suffered from poor stability properties, the exponential EM scheme has shown high performance in accuracy, computational costs and stability.

References

[1] A. Abdulle. Fourth order Chebyshev methods with recurrence relation. *SIAM J. Sci. Comput.*, **23**(**6**):2041–2054, 2002.

[2] A. Abdulle and S. Cirilli. S-ROCK: Chebyshev methods for stiff stochastic differential equations. *SIAM J. Sci. Comput.*, **30**(**2**):997–1014, 2008.

[3] A. Abdulle and T. Li. S-ROCK methods for stiff Itô SDEs. *Commun. Math. Sci.*, **6**(**4**):845–868, 2008.

[4] A. Abdulle and A.A. Medovikov. Second order Chebyshev methods based on orthogonal polynomials. *Numer. Math.*, **90**:1–18, 2001.

[5] L. Arnold. *Stochastic Differential Equations: Theory and Applications*. John Wiley & Sons, New York, 1974.

[6] C. Bayer, A. Szepessy, and R. Tempone. Adaptive weak approximation of reflected and stopped diffusions. *Monte Carlo Methods Appl.*, **16**(**1**):1–67, 2010.

[7] R. Biscay, J.C. Jimenez, J.J. Riera, and Valdes P.A. Local linearization method for numerical solution of stochastic differential equations. *Ann. Inst. Statist. Math.*, **48**(**4**):631–644, 1996.

[8] T. Brennan, M. Fink, and B. Rodriguez. Multiscale modelling of drug-induced effects on cardiac electrophysiological activity. *Eur. J. Pharm. Sci.*, **36**(**1**):62–77, 2009.

[9] J.C. Butcher. *Numerical Methods for Ordinary Differential Equations*. John Wiley & Sons, Chichester, second edition, 2008.

[10] F. Carbonell, J.C. Jimenez, and R.J. Biscay. Weak local linear discretizations for stochastic differential equations: Convergence and numerical schemes. *J. Comput. Appl. Math.*, **197**(**2**):578–596, 2006.

[11] Y. Chen and X. Ye. Projection onto a simplex. e-print, 2011. arXiv:1101.6081v2.

[12] de la Cruz, R.J. Biscay, J.C. Jimenez, F. Carbonell, and T. Ozaki. High order local linearization methods: An approach for constructing A-stable explicit schemes for stochastic differential equations with additive noise. *BIT*, **50**(**3**):509–539, 2010.

[13] C. Dangerfield, D. Kay, and K. Burrage. Modeling ion channel dynamics through reflected stochastic differential equations. *Phys. Rev. E*, **85**:051907, 15 pp., 2012.

[14] B.L. Ehle and J.D. Lawson. Generalized runge-kutta processes for stiff initial-value problems. *IMA J. Appl. Math.*, **16**(**1**):11–21, 1975.

[15] D.T. Gillespie. The chemical Langevin equation. *J. Chem. Phys.*, **113**(**1**):297–306, 2000.

[16] D.J. Higham. A-stability and stochastic mean-square stability. *BIT*, **40**(**2**):404–409, 2000.

[17] M. Hochbruck, C. Lubich, and H. Selhofer. Exponential integrators for large systems of differential equations. *SIAM J. Sci. Comput.*, **19**(**5**):1552–1574, 1998.

[18] M. Hochbruck and A. Ostermann. Explicit exponential Runge-Kutta methods for semilinear parabolic problems. *SIAM J. Numer. Anal.*, **43**(**3**):1069–1090, 2005.

[19] M. Hochbruck and A. Ostermann. Exponential integrators. *Acta Numer.*, **19**:209–286, 2010.

[20] S. Ilie and M. Morshed. Automatic simulation of the chemical Langevin equation. *Appl. Math.*, **4**(**1A**):235–241, 2013.

[21] A. Jentzen and Kloeden E. Overcoming the order barrier in the numerical approximation of stochastic partial differential equations with additive space-time noise. In *Proc. R. Soc. Lond. Ser. A Math. Phys. Eng. Sci. 465*, pages 649–667, 2009.

[22] J.C. Jimenez. A simple algebraic expression to evaluate the local linearization schemes for stochastic differential equations. *Appl. Math. Lett.*, **15**(**6**):775–780, 2002.

[23] J.C. Jimenez and de la Cruz. Convergence rate of strong local linearization schemes for stochastic differential equations with additive noise. *BIT*, **52**(**2**):357–382, 2012.

[24] J.C. Jimenez, I. Shoji, and T. Ozaki. Simulation of stochastic differential equations through the local linearization method. a comparative study. *J. Stat. Phys.*, **94**(**3-4**):587–602, 1999.

[25] J. Kiehn, A.E. Lacerda, and A.M. Brown. Pathways of herg inactivation. *Am. J. Physiol. Heart Circ. Physiol.*, **277**(**1**):199–210, 1999.

[26] P.E. Kloeden and E. Platen. *Numerical Solution of Stochastic Differential Equations*. Springer, New York, 1999. Corrected Third Printing.

[27] Y. Komori and K. Burrage. Weak second order S-ROCK methods for Stratonovich stochastic differential equations. *J. Comput. Appl. Math.*, **236**(**11**):2895–2908, 2012.

[28] Y. Komori and K. Burrage. Strong first order S-ROCK methods for stochastic differential equations. *J. Comput. Appl. Math.*, **242**:261–274, 2013.

[29] B. Mélykúti, K. Burrage, and K.C Zygalakis. Fast stochastic simulation of biochemical reaction systems by alternative formulations of the chemical langevin equation. *J. Chem. Phys.*, **132**(**16**):164109, 2010.

[30] C.M. Mora. Weak exponential schemes for stochastic differential equations with additive noise. *IMA J. Numer. Anal.*, **25**(**3**):486–506, 2005.

[31] R. Pettersson. Approximations for stochastic differential equations with reflecting convex boundaries. *Stochastic Process. Appl.*, **59**(**2**):295–308, 1995.

[32] D. Pope. An exponential method of numerical integration of ordinary differential equations. *Comm. ACM*, **6**(**8**):491–493, 1963.

[33] A. Rößler. Runge-Kutta methods for the strong approximation of solutions of stochastic differential equations. *SIAM J. Numer. Anal.*, **48**(**3**):922–952, 2010.

[34] I. Shoji. A note on convergence rate of a linearization method for the discretization of stochastic differential equations. *Commun. Nonlinear Sci. Numer. Simul.*, **16**(7):2667–2671, 2011.

[35] A. V. Skorohod. Stochastic equations for diffusion processes with a boundary. *Theory Probab. Appl.*, **6**:287–298, 1961.

[36] A. V. Skorohod. Stochastic equations for diffusion processes with boundaries. II. *Theory Probab. Appl.*, **7**:5–25, 1962.

[37] H. Tanaka. Stochastic differential equations with reflecting boundary condition in convex regions. *Hiroshima Math. J.*, **9**(1):163–177, 1979.

[38] P.J. van der Houwen and B.P. Sommeijer. On the internal stability of explicit m-stage Runge-Kutta methods for large m-values. *Z. Angew. Math. Mech.*, **60**:479–485, 1980.